Iterative Three-Dimensional Transonic Wing Design Using Integral Equations

S. Takanashi*
National Aerospace Laboratory, Tokyo, Japan

A practical design method is presented for three-dimensional transonic wings with prescribed pressure distributions. The method is based on an iterative "residual-correction" concept. The residual, defined as the difference between the computed and the prescribed pressure distributions at each iteration step, is determined by the use of an existing direct analysis code for a transonic wing with or without the body. The wing geometry correction to compensate for the residual can be approximately obtained from the inverse solution code developed in the present study. The inverse (correction) problem is mathematically reduced to a Dirichlet boundary value problem that is solved here by the aid of the transonic integral equation method. Some of the design results are also presented for transonic swept wings.

Nomenclature

C_p	= pressure coefficient
$\bar{f}, f$	= wing surface coordinates
$\bar{H}, \bar{Q}, \bar{S}$, H, Q, S	= higher-order terms in transonic small disturbance series expansion
i, j	= indices (Fig. 1)
I, J	= max(i), max(j)
K	= transonic similarity parameter
M_∞	= freestream Mach number
R	= decay function, Eq. (27)
S_v	= vortex sheet
S_w	= wing mean plane
S_{wv}	= $S_w + S_v$
x_i^j, y_j	= x and y coordinates of a small panel, respectively (Fig. 1)
$x_{i+1/2}^j$	= $\frac{1}{2}(x_{i+1}^j + x_i^j)$ $(i = 1,2,\ldots,I-1)$
x_{LE}	= x coordinate of leading edge = $x_{1/2}^j$
x_{TE}	= x coordinate of trailing edge = $x_{I+1/2}^j$
$(\bar{x},\bar{y},\bar{z})$, (x,y,z)	= Cartesian coordinate systems
β	= $\sqrt{1-M_\infty^2}$
γ	= ratio of specific heats
$\Delta(\ )$	= perturbation quantity
$\bar{\phi}, \phi$	= perturbation velocity potentials
ψ	= kernel function, Eq. (17)
$\overline{(\ )}$	= value in physical space

Superscripts and Subscripts

$(\ )^s, (\ )_s$	= symmetric parts
$(\ )^a, (\ )_a$	= antisymmetric parts
$(\ )_+, (\ )_-$	= values on upper and lower surfaces of wing, respectively

Introduction

STIMULATED by the rapid progress in computer technology, great advances have recently been made in computational transonic aerodynamics. Especially in the field of the direct problem, it has become feasible to compute numerically even the transonic flow around an almost full configuration of a realistic aircraft, in so far as the flow is governed by inviscid transonic equations (e.g., see Refs. 1 and 2). Since a number of reliable and accurate direct analysis codes are now available, wing design methods based on the numerical optimization concept (originally proposed by Hicks et al.[3] in 1976) have been extensively investigated in recent years. In this optimization technique, a wing section shape with, for example, minimal total drag under some constraints (such as a specified lift coefficient and/or a specified maximum thickness ratio) is sought by means of the alternating iterative use of two computer codes—an existing flow analysis code and a numerical minimization code. Although such an optimization approach may have a bright future as a powerful design tool, it requires excessive computation time even when using the latest computer system, particularly if a realistic three-dimensional wing configuration is desired.

On the other hand, there exist "inverse methods" of wing design in which the wing surface geometry can be determined so as to realize the prescribed (favorable) pressure distribution. Attempts to solve a three-dimensional inverse problem of this type on the basis of the full potential equation were made by Henne[4] for a wing-alone configuration and by Shankar[5] for a wing/body combination. While their formulations are considerably different from each other, the essential feature common to both approaches is to iteratively solve a Dirichlet boundary value problem in which the velocity potential derived from a specified pressure or velocity distribution is imposed as a boundary condition on the transient wing surface at each iteration step. The codes used in Refs. 4 and 5 were obtained by reformulating and modifying the FLO-22[6] and FLO-30[7] analysis codes, respectively, in order to accommodate the Dirichlet boundary conditions.

In the present paper, an alternative approach is proposed for the same three-dimensional transonic wing design problem. The present method is based on an iterative "residual-correction" procedure similar to those used by Barger and Brooks,[8] Davis,[9] and McFadden[10] in their work on the design of a two-dimensional transonic airfoil. The advantage of this approach is that only minimal effort in developing the geometry correction code is needed to compensate for the pressure residual, while an analysis code is retained in its original form and can be treated solely as a "black box." As a result, the analysis code can be easily replaced whenever a more advanced code becomes available.

Presented as Paper 84-2155 at the AIAA 2nd Applied Aerodynamics Conference, Seattle, Wash., Aug. 21-23, 1984; received Sept. 24, 1984; revision received Feb. 13, 1985.

*Senior Research Scientist. Member AIAA.

The geometry correction problem is formulated in the form of three-dimensional transonic integral equations that are discretized and solved numerically. The mathematical formulation, numerical solution method, iteration procedure, and design results are described in the following sections.

Integral Equation Formulation for the Inverse Problem

Let the three-dimensional full potential equation be written in terms of the perturbation velocity potential as

$$(1-M_\infty^2)\bar{\phi}_{\bar{x}\bar{x}}+\bar{\phi}_{\bar{y}\bar{y}}+\bar{\phi}_{\bar{z}\bar{z}}=K\frac{\partial}{\partial\bar{x}}(\tfrac{1}{2}\bar{\phi}_{\bar{x}}^2)+\bar{H} \tag{1}$$

The flow tangency condition on the wing may be written as

$$\bar{\phi}_{\bar{z}}(\bar{x},\bar{y},\pm 0)=\bar{f}'_{\pm}(\bar{x},\bar{y})+\bar{Q} \tag{2}$$

where $\bar{f}'_{\pm}(\bar{x},\bar{y})=(\partial/\partial\bar{x})\bar{f}_{\pm}(\bar{x},\bar{y})$.

The pressure coefficients on the wing surfaces are expressed as

$$C_{p\pm}(\bar{x},\bar{y})=-2\bar{\phi}_{\bar{x}}(\bar{x},\bar{y},\pm 0)+\bar{S} \tag{3}$$

Introducing new variables

$$x=\bar{x},\quad y=\beta\bar{y},\quad z=\beta\bar{z},\quad \phi(x,y,z)=(K/\beta^2)\bar{\phi}(\bar{x},\bar{y},\bar{z}) \tag{4}$$

Eqs. (1-3) become, respectively,

$$\phi_{xx}+\phi_{yy}+\phi_{zz}=\frac{\partial}{\partial x}(\tfrac{1}{2}\phi_x^2)+H \tag{5}$$

$$\phi_z(x,y,\pm 0)=f'_{\pm}(x,y)+Q \tag{6}$$

$$C_{p\pm}\left(x,\frac{y}{\beta}\right)=-2\frac{\beta^2}{K}\phi_x(x,y,\pm 0)+S \tag{7}$$

where the function $f_{\pm}(x,y)$ is introduced for convenience and defined as

$$f_{\pm}(x,y)=(K/\beta^3)\bar{f}_{\pm}(\bar{x},\bar{y}) \tag{8}$$

The objective of the present investigation is to obtain the wing geometry $f_{\pm}(x,y)$ that realizes a specified pressure distribution $C_{p\pm}(x,y/\beta)$. The most common approach is the direct solution of the partial differential equation (5) subject to the boundary condition [Eq. (7)]. In the present paper, however, an iterative "residual-correction" method is adopted with the view to developing a more general design procedure with a wide range of applications.

Assume that the solution $\phi(x,y,z)$ of Eq. (5) for an initial wing geometry $f_{\pm}(x,y)$ has been obtained by means of an existing full potential flow solver. If a perturbation $\Delta\phi(x,y,z)$ is further introduced in this known flow, the governing equation becomes

$$(\phi_{xx}+\Delta\phi_{xx})+(\phi_{yy}+\Delta\phi_{yy})+(\phi_{zz}+\Delta\phi_{zz})$$
$$=\frac{\partial}{\partial x}[\tfrac{1}{2}(\phi_x+\Delta\phi_x)^2]+H+\Delta H \tag{9}$$

with the tangency condition

$$\phi_z(x,y,\pm 0)+\Delta\phi_z(x,y,\pm 0)=f'_{\pm}(x,y)+\Delta f'_{\pm}(x,y)+Q+\Delta Q \tag{10}$$

and the boundary condition

$$C_{p\pm}\left(x,\frac{y}{\beta}\right)+\Delta C_{p\pm}\left(x,\frac{y}{\beta}\right)$$
$$=-2\frac{\beta^2}{K}[\phi_x(x,y,\pm 0)+\Delta\phi_x(x,y,\pm 0)]+S+\Delta S \tag{11}$$

If the transonic similarity parameter $K(\gamma,M_\infty)$ in Eq. (1) is appropriately chosen—in other words, calibrated depending on the analysis code—and the perturbation $\Delta\phi(x,y,z)$ is small, then the higher-order terms ΔH, ΔQ, and ΔS may be assumed to be small even when shock waves are present. The reason is that the transonic small-disturbance theory has been demonstrated by many investigators to provide a good approximation of the full potential flow over the fairly wide range of variations in wing geometries, planform shapes, and freestream Mach numbers. Therefore, putting $\Delta H=\Delta Q=\Delta S=0$, we get the perturbation equations

$$\Delta\phi_{xx}+\Delta\phi_{yy}+\Delta\phi_{zz}=\frac{\partial}{\partial x}[\tfrac{1}{2}(\phi_x+\Delta\phi_x)^2-\tfrac{1}{2}\phi_x^2] \tag{12}$$

$$\Delta\phi_z(x,y,\pm 0)=\Delta f'_{\pm}(x,y) \tag{13}$$

$$\Delta C_{p\pm}\left(x,\frac{y}{\beta}\right)=-2\frac{\beta^2}{K}\Delta\phi_x(x,y,\pm 0) \tag{14}$$

Since the body geometry remains unaltered in the present wing design procedure, the spanwise velocity component $\Delta\phi_y(x,y,z)$ may be assumed to be small on the plane $y=0$ that contains the wing root section. Hence, putting $\Delta\phi_y(x,0,z)=0$, the perturbation flow $\Delta\phi(x,y,z)$ for even the wing/body combination can be considered to be symmetrical with respect to this plane, just as in the case of the wing-alone configuration.

By application of Green's theorem (see, e.g., Ref. 11), Eq. (12) can be converted into the following integrodifferential equation:

$$\Delta\phi(x,y,z)=-\frac{1}{4\pi}\iint_{S_{wv}}\{\psi(x,y,z;\xi,\eta,0)$$
$$\times[\Delta\phi_\zeta(\xi,\eta,+0)-\Delta\phi_\zeta(\xi,\eta,-0)]$$
$$-\psi_\zeta(x,y,z;\xi,\eta,0)[\Delta\phi(\xi,\eta,+0)-\Delta\phi(\xi,\eta,-0)]\}\mathrm{d}\xi\mathrm{d}\eta$$
$$+\frac{1}{4\pi}\int_{-\infty}^{\infty}\int_{-\infty}^{\infty}\int_{-\infty}^{\infty}\psi_\xi(x,y,z;\xi,\eta,\zeta)\chi(\xi,\eta,\zeta)\mathrm{d}\xi\mathrm{d}\eta\mathrm{d}\zeta \tag{15}$$

where

$$\chi(x,y,z)=\tfrac{1}{2}[(\phi_x+\Delta\phi_x)^2-\phi_x^2] \tag{16}$$

$$\psi(x,y,z;\xi,\eta,\zeta)=[(x-\xi)^2+(y-\eta)^2+(z-\zeta)^2]^{-\frac{1}{2}} \tag{17}$$

and the principal value defined by Oswatitch[12] is used here for the triple integral in Eq. (15), viz.,

$$\int_{-\infty}^{\infty}\int_{-\infty}^{\infty}\int_{-\infty}^{\infty}(\quad)\mathrm{d}\xi\mathrm{d}\eta\mathrm{d}\zeta=\lim_{\epsilon\to 0}\left\{\int_{-\infty}^{\infty}\int_{-\infty}^{\infty}\right.$$
$$\left.\times\left[\int_{-\infty}^{x-\epsilon}(\quad)\mathrm{d}\xi+\int_{x+\epsilon}^{\infty}(\quad)\mathrm{d}\xi\right]\mathrm{d}\eta\mathrm{d}\zeta\right\} \tag{18}$$

Differentiating both sides of Eq. (15) with respect to x and adding the value of resulting $\Delta\phi_x(x,y,z)$ at $z=+0$ to that at

$z=-0$, we get

$$\Delta u_s(x,y) = -\frac{1}{2\pi}\iint_{S_w}\psi_x(x,y,0;\xi,\eta,0)\Delta w_s(\xi,\eta)\,d\xi d\eta$$
$$+\chi_s(x,y)+\frac{1}{4\pi}\int_{-\infty}^{\infty}\int_{-\infty}^{\infty}\int_{-\infty}^{\infty}\psi_{\xi x}(x,y,0;\xi,\eta,\zeta)$$
$$\times[\chi(\xi,\eta,\zeta)+\chi(\xi,\eta,-\zeta)]\,d\xi d\eta d\zeta \tag{19}$$

where

$$\chi_s(x,y) = \chi(x,y,+0)+\chi(x,y,-0) \tag{20}$$
$$\Delta u_s(x,y) = \Delta\phi_x(x,y,+0)+\Delta\phi_x(x,y,-0) \tag{21}$$
$$\Delta w_s(x,y) = \Delta\phi_z(x,y,+0)-\Delta\phi_z(x,y,-0) \tag{22}$$

Similarly, differentiating both sides of Eq. (15) with respect to z, adding the value of $\Delta\phi_z(x,y,z)$ at $z=+0$ to that at $z=-0$, and using an integration by parts, we get

$$\Delta w_a(x,y) = \frac{1}{2\pi}\iint_{S_w}\frac{\Delta u_a(\xi,\eta)}{(y-\eta)^2}$$
$$\times\left[1+\frac{x-\xi}{\sqrt{(x-\xi)^2+(y-\eta)^2}}\right]d\xi d\eta$$
$$+\frac{1}{4\pi}\int_{-\infty}^{\infty}\int_{-\infty}^{\infty}\int_{-\infty}^{\infty}\psi_{\xi z}(x,y,0;\xi,\eta,\zeta)$$
$$\times[\chi(\xi,\eta,\zeta)-\chi(\xi,\eta,-\zeta)]\,d\xi d\eta d\zeta \tag{23}$$

where

$$\Delta u_a(x,y) = \Delta\phi_x(x,y,+0)-\Delta\phi_x(x,y,-0) \tag{24}$$
$$\Delta w_a(x,y) = \Delta\phi_z(x,y,+0)+\Delta\phi_z(x,y,-0) \tag{25}$$

Evaluation of the triple integrals on the right-hand sides of Eqs. (19) and (23) requires a knowledge of $\chi(x,y,z)$ over the entire flowfield. To cope with this problem, a decay function similar to that used by Nørstrud[13] was employed here to approximate the variation of $\phi_x(x,y,z)$ with z as follows:

$$\phi_x(x,y,z) = \phi_x(x,y,\pm 0)\exp[\mp R_\pm(x,y)z] \tag{26}$$

where

$$R_\pm(x,y) = \mathrm{abs}[f''_\pm(x,y)/\phi_x(x,y,\pm 0)] \tag{27}$$

with $f''_\pm(x,y)=(\partial^2/\partial x^2)f_\pm(x,y)$.

Since the relation $\phi_z(x,y,\pm 0)=f'_\pm(x,y)$ holds approximately [see Eq. (6)], the decay function defined above satisfies approximately the irrotationality condition $\phi_{xz}=\phi_{zx}$ on the wing surfaces. Therefore, assuming the relation

$$\Delta\phi_x(x,y,z)\sim\Delta\phi_x(x,y,\pm 0)\exp[\mp R_\pm(x,y)z] \tag{28}$$

the analytical expression for $\chi(x,y,z)$ becomes

$$\chi(x,y,z) = \tfrac{1}{2}\{[\phi_x(x,y,z)+\Delta\phi_x(x,y,z)]^2-\phi_x^2(x,y,z)\}$$
$$=\chi(x,y,\pm 0)\exp[\mp 2R_\pm(x,y)z] \tag{29}$$

Substituting Eq. (29) into Eqs. (19) and (23) and neglecting the minor effects induced from the points upstream and downstream of the wing, we get

$$\Delta u_s(x,y) = -\frac{1}{2\pi}\iint_{S_w}\psi_x(x,y,0;\xi,\eta,0)\Delta w_s(\xi,\eta)\,d\xi d\eta$$
$$+\chi_s(x,y)+\frac{1}{2\pi}\iint_{S_w}[I_s(x,y;\xi,\eta,+0)\chi(\xi,\eta,+0)$$
$$+I_s(x,y;\xi,\eta,-0)\chi(\xi,\eta,-0)]\,d\xi d\eta \tag{30}$$

$$\Delta w_a(x,y) = \frac{1}{2\pi}\iint_{S_w}\frac{\Delta u_a(\xi,\eta)}{(y-\eta)^2}$$
$$\times\left[1+\frac{x-\xi}{\sqrt{(x-\xi)^2+(y-\eta)^2}}\right]d\xi d\eta$$
$$+\frac{1}{2\pi}\iint_{S_w}[I_a(x,y;\xi,\eta,+0)\chi(\xi,\eta,+0)$$
$$-I_a(x,y;\xi,\eta,-0)\chi(\xi,\eta,-0)]\,d\xi d\eta \tag{31}$$

where

$$I_s(x,y;\xi,\eta,\pm 0) = \int_0^\infty\psi_{\xi x}(x,y,0;\xi,\eta,\zeta)\exp[-2R_\pm(\xi,\eta)\zeta]\,d\zeta \tag{32}$$

$$I_a(x,y;\xi,\eta,\pm 0) = \int_0^\infty\psi_{\xi z}(x,y,0;\xi,\eta,\zeta)\exp[-2R_\pm(\xi,\eta)\zeta]\,d\zeta \tag{33}$$

Hence, the complicated three-dimensional integral equations are now reduced to the far simpler two-dimensional analogs.

The primary objective considered here is to determine the amount of the wing surface correction $\Delta\bar{f}_\pm(\bar{x},\bar{y})$, or equivalently $\Delta f_\pm(x,y)$, corresponding to the pressure difference $\Delta C_{p\pm}(x,y/\beta)$ between the specified and calculated pressures. For convenience, the (transformed) surface correction function $\Delta f_\pm(x,y)$ is split into symmetric $\Delta f_s(x,y)$ and antisymmetric $\Delta f_a(x,y)$ parts of the (transformed) surface coordinates,

$$\Delta f_s(x,y) = \Delta f_+(x,y)-\Delta f_-(x,y) \tag{34}$$
$$\Delta f_a(x,y) = \Delta f_+(x,y)+\Delta f_-(x,y) \tag{35}$$

Since $\Delta f'_a(x,y)=\Delta w_a(x,y)$ from Eqs. (13), (25), and (35), the antisymmetric part can be uniquely determined by direct evaluation of the right-hand side of Eq. (31). On the other hand, the symmetric part $\Delta f'_s(x,y)$, or equivalently $\Delta w_s(x,y)$, included in the integrand of the first integral in Eq. (30) must be implicitly solved. Furthermore, a rather troublesome problem occurs, since Eq. (30) for given $\Delta u_s(x,y)$, $\chi_s(x,y)$, $\chi(x,y,\pm 0)$, and $R_\pm(x,y)$ does not have a unique solution unless an additional condition is imposed. However, this difficulty can be resolved here by setting the following closure condition at the trailing edge:

$$\int_{x_{\mathrm{LE}(y)}}^{x_{\mathrm{TE}(y)}}\Delta f'_s(x,y)\,dx=0 \quad\text{or}\quad \int_{x_{\mathrm{LE}(y)}}^{x_{\mathrm{TE}(y)}}\Delta w_s(x,y)\,dx=0 \tag{36}$$

This closure condition is physically important in that the trailing-edge thickness of the current wing during iterations is always kept equal to that of the initial wing. However, the trailing-edge closure condition defined above does not necessarily mean that the resulting contour has no crossing at any x, $x_{\mathrm{LE}}<x<x_{\mathrm{TE}}$. If this crossing does occur, the specified

pressure distribution must inevitably be modified in order to obtain a physically meaningful wing.

Numerical Evaluation of the Integrals

In order to facilitate the numerical evaluation of the single integrals appearing in Eqs. (32) and (33), the range of integration with respect to ζ is divided into a finite number of subintervals. Assuming that $R_{\pm}(\xi,\eta)\zeta$ is constant on each subinterval, Eqs. (32) and (33) can be expressed as

$$I_s(x,y;\xi,\eta,\pm 0) = \sum_{n=0}^{K} \exp[-2R\pm(\xi,\eta)\zeta_n] \times \int_{\zeta_\eta - \frac{1}{2}\Delta\zeta_{n-1}}^{\zeta_\eta + \frac{1}{2}\Delta\zeta_n} \psi_{\xi x}(x,y,0;\xi,\eta,\zeta)\mathrm{d}\zeta \tag{37}$$

$$I_a(x,y;\xi,\eta,\pm 0) = \sum_{n=0}^{K} \exp[-2R_{\pm}(\xi,\eta)\zeta_n] \times \int_{\zeta_\eta - \frac{1}{2}\Delta\zeta_{n-1}}^{\zeta_\eta + \frac{1}{2}\Delta\zeta_n} \psi_{\xi z}(x,y,0;\xi,\eta,\zeta)\mathrm{d}\zeta \tag{38}$$

where

$$\zeta_n = \frac{a[n/(K+1)]}{\{1-[n/(K+1)]^2\}^2}, \qquad n=0,1,2,\ldots,K \tag{39}$$

$$\Delta\zeta_n = \zeta_{n+1} - \zeta_n, \qquad \Delta\zeta_{-1} \equiv 0 \tag{40}$$

and where a is an arbitrary positive parameter and the total number of nodal points for a fixed point (ξ,η) is $K+1$.

As shown in Fig. 1, the wing surfaces are also divided into small rectangular panels of $I(2J+1)$ on each of which $\Delta u_s(x,y)$, $\Delta u_a(x,y)$, $\chi_s(x,y)$, $\chi(x,y,\pm 0)$, $R_{\pm}(x,y)$, and $\Delta w_a(x,y)$ are assumed to be constant, while $\Delta w_s(x,y)$ is assumed to vary linearly in the chordwise direction but to be constant in the other direction. These assumptions make it easy to evaluate the surface integrals numerically in Eqs. (30) and (31). The total number of unknown quantities $\Delta w_s(x^j_{i-\frac{1}{2}}, y_j)$ is $I+1$ at each span station y_j, whereas the total number of points (x^j_i, y_j) at which the known quantities such as Δu_s are defined, is I. Hence, the uniqueness of the solution can be guaranteed by imposing one additional condition, i.e., the trailing-edge closure condition of Eq. (36). The discretized form of Eq. (36) can be expressed as

$$\sum_{i=1}^{I} \tfrac{1}{2}[\Delta w_s(x^j_{i-\frac{1}{2}}, y_j) + \Delta w_s(x^j_{i+\frac{1}{2}}, y_j)](x^j_{i+\frac{1}{2}} - x^j_{i-\frac{1}{2}}) = 0 \tag{41}$$

Recalling that the perturbed flow $\Delta\phi(x,y,z)$ due to the pressure residual $\Delta C_{p\pm}(x,y/\beta)$ may be considered to be symmetrical (regardless of the presence of body) with respect to the plane $y=0$, the final expressions of Eqs. (30) and (31) in discretized form are as follows:

$$\Delta u_s(x^j_i,y_j) = \sum_{k=1}^{I+1}\sum_{m=0}^{J} \mu^s_{ijkm}\Delta w_s(x^m_{k-\frac{1}{2}}, y_m) + \chi_s(x^j_i, y_j) + \sum_{k=1}^{I}\sum_{m=0}^{J} [\nu^s_{ijkm}\chi(x^m_k,y_m,+0) + \hat{\nu}^s_{ijkm}\chi(x^m_k,y_m,-0)] \tag{42}$$

$$\Delta w_a(x^j_i,y_j) = \sum_{k=1}^{I}\sum_{m=0}^{J} \mu^a_{ijkm}\Delta u_a(x^m_k,y_m) + \sum_{k=1}^{I}\sum_{m=0}^{J} [\nu^a_{ijkm}\chi(x^m_k,y_m,+0) - \hat{\nu}^a_{ijkm}\chi(x^m_k,y_m,-0)] \tag{43}$$

where the coefficients

$$\mu^s_{ijkm},\ \mu^a_{ijkm},\ \nu^s_{ijkm},\ \nu^a_{ijkm},\ \hat{\nu}^s_{ijkm},\ \text{and}\ \hat{\nu}^a_{ijkm}$$

are the integral representations over each small panel (k,m). The full expressions are omitted here because they are lengthy and tedious.

The antisymmetric part Δw_a can be readily determined by the direct evaluation of the right-hand side of Eq. (43). On the other hand, a system of $(I+1)(J+1)$ linear equations for the symmetric part Δw_s is solved by standard techniques such as the Gaussian elimination method. Consequently, the correction Δf in the wing surface is obtained by numerically integrating Δw_s and Δw_a with respect to x.

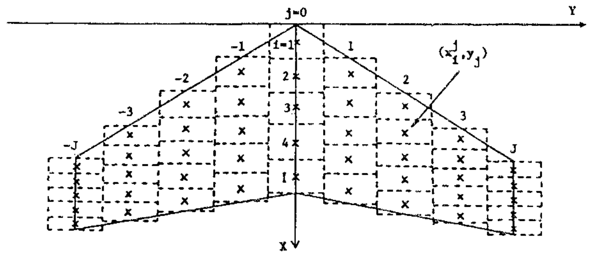

Fig. 1 Paneling of the wing surface for numerical solution of the integral equations.

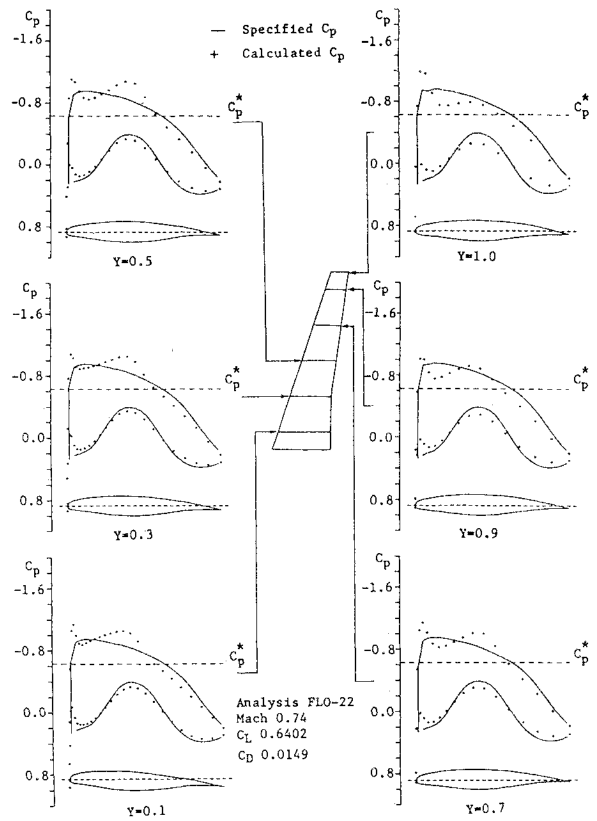

Fig. 2 Starting wing geometry and corresponding pressure distributions as well as specified (target) pressure distributions.

Procedure of Iteration

The basic procedure of iteration for the wing design is described in this section. The iteration process is: 1) the flowfield is solved for an initial wing f by a direct analysis code that provides the initial pressure distribution C_p; and 2) the inverse correction code is used to obtain the value Δf of the geometric correction corresponding to the pressure difference ΔC_p between the actually computed C_p at the first step and a specified pressure distribution C_{ps}. So long as the higher-order terms ΔH, ΔQ, and ΔS are small, Δf can provide a good approximation of the exact amount of correction for the initial

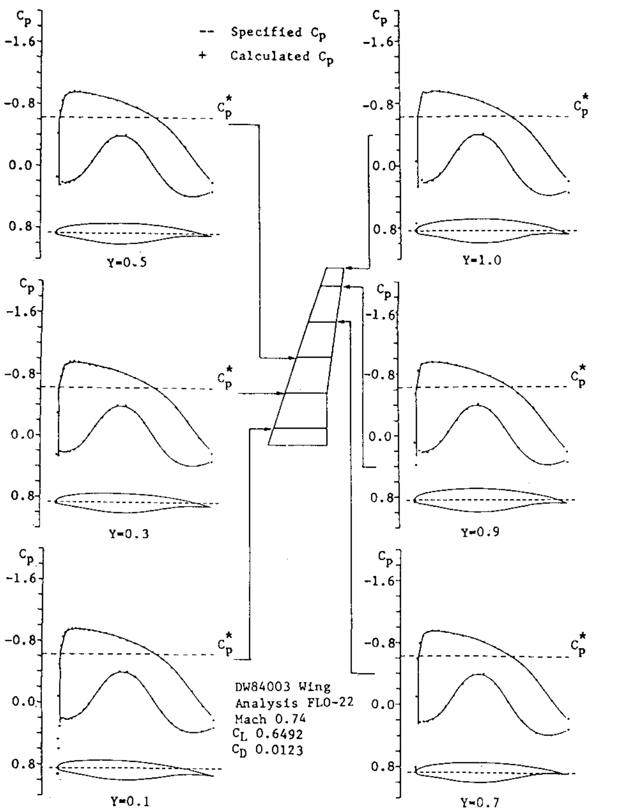

Fig. 3 Designed wing geometry and pressure distributions after 10 iterations.

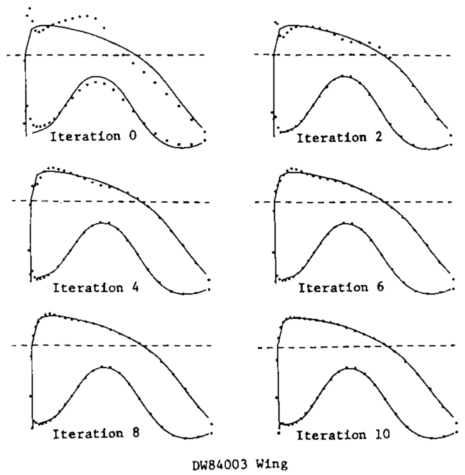

Fig. 4 Improvement of pressure distribution at 10% semispan at each iteration step.

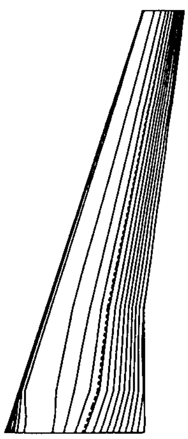

Fig. 5 Isobar pattern on upper surface of wing DW84003.

wing geometry. Thus, a new wing geometry is obtained that, in turn, can be used as the second set of input data to the analysis code. The same process is repeated until convergence is achieved in the sense that the calculated pressure distribution agrees with the prescribed one within a specified amount of tolerance.

This procedure requires neither restrictions on the formulation nor a numerical solution scheme for the analysis code. The only requirement is that the flow solver calculate the pressure distribution on the corrected wing surface, since the design code is completely independent of the analysis code. Therefore, any analysis code for a three-dimensional transonic wing with or without a body can be employed using the present procedure.

Computed Results

To show the validity of the present design procedure, only a few examples of the computed results are presented. FLO-22 was at first used as a direct analysis code for the nonconservative finite difference equations derived from the three-dimensional transonic full potential equations.

A transonic swept-wing design for a transport airplane was attempted. The freestream Mach number was specified as $M_\infty = 0.74$ and the wing planform fixed at 9.92 aspect ratio, 18.4 deg leading-edge swept angle, 0.3 taper ratio, and 30% semispan trailing-edge kink station. The original wing section profiles and the calculated pressure distribution, together with the specified (target) pressure distribution, are shown in Fig. 2. The target pressure distribution chosen here as the first test case is characterized by its particular isobar pattern. That is, the specified chordwise pressure distributions are the same at any span station between the wing root and tip, so that the straight-line isobar pattern is realized over the entire wing surface.

The target pressure distribution selected in the present example is based on the results of a two-dimensional airfoil design. The airfoil characteristics were investigated by airfoil analysis codes and verified by high Reynolds number wind tunnel tests.

In the present example, the thickness of the wing section at the root station increased monotonically as the iteration proceeded. Ultimately, the numerical solution of the FLO-22 code became unstable. To prevent this instability, the root section profile was fixed throughout the iterations. Ten iterations were required before the target pressure distribution was realized, see Fig. 3. Figure 4 shows the improvement in the pressure distribution at each iteration step at a selected station of 10% semispan. Pressure distributions at the other span stations converge similarly, but will not be shown here. As shown in Fig. 5, a practically straight-line isobar is realized, except in very close proximity of the root section. The lift coefficient is 0.65 and the drag coefficient 0.0123.

For the present design case, a set of small rectangular 20×6 panels was used for the evaluation of the integrals, while the FLO-22 code was run with medium mesh of $96 \times 12 \times 16$. The computation time for the inverse design mode was negligibly small compared with the time required for the direct analysis mode. The total computation time for 10 iterations was 15 min on FACOM M-380 at National Aerospace Laboratory.

The adoption of other full potential codes has been successfully attempted. For example, Fig. 6 shows the design results for a wing/body combination using the Jameson-Cauchey[14] analysis code FLO-27. The present example is also a case of a mixed inverse/direct problem, namely the wing sections are in a design mode at specified span stations (i.e., 30-90% semispan), while the remaining sections (as well as the body) are in the analysis mode. The most important feature of the present target distributions with spanwise uniformity is that they include rather strong shock waves on the upper surface of the wing. The target pressure distributions were fairly well realized with three iterations, although a small disagreement is noticed near the shock locations.

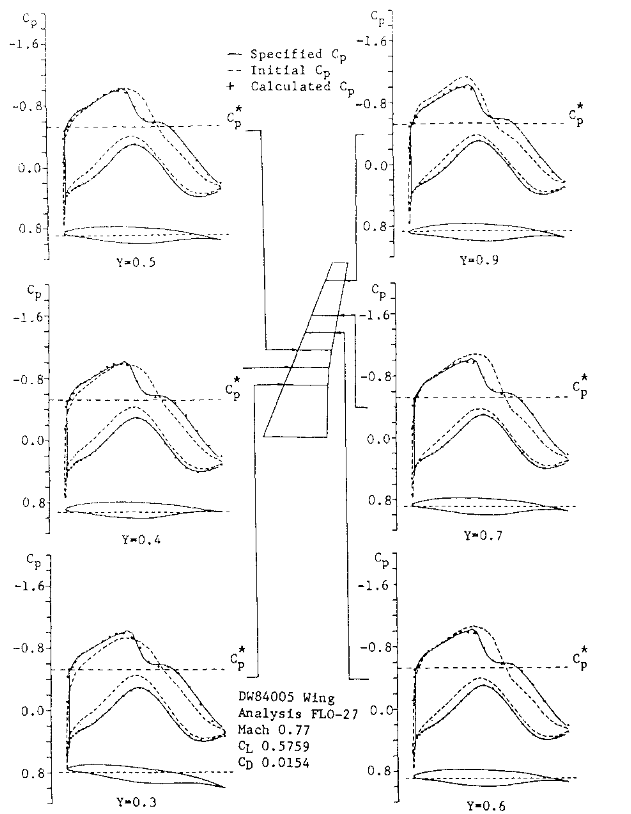

Fig. 6 Design results for target pressure distributions with shock waves after three iterations.

Conclusions

A general and versatile design method has been developed for three-dimensional transonic wings with a prescribed pressure distribution.

The most important features of the present method are summarized as follows:

1) The integral equation method was extended and modified for the purpose of solving the inverse problem.

2) An existing direct analysis code and the integral inverse design code are alternately used in the iterative "residual-correction" procedure.

3) The analysis code is treated solely as a "black box." It is easily exchangeable whenever a new code becomes available.

4) The trailing-edge closure is automatically taken into account at each (design) iteration step.

5) Convergence is satisfactory from the practical point of view.

6) Two typical design examples computed by the present method, using, FLO-22 and FLO-27 as the analysis codes, were presented for transonic swept wings with specified pressure distributions.

Acknowledgments

The author would like to thank Ms. T. Iida, Ms. H. Toyota, and Ms. J. Fukuyama for developing the computer codes for the present design work and his colleagues Dr. N. Kamiya and Dr. N. Hirose for their encouragement and helpful discussions.

References

[1]Boppe, C. W. and Stern, M. A., "Simulated Transonic Flows for Aircraft with Nacelles, Pylons, and Winglets," AIAA Paper 80-0130, 1980.

[2]Jameson, A. and Baker, T. J., "Solution of the Euler Equations for Complex Configurations," AIAA Paper 83-1929, 1983.

[3]Hicks, R. M., Vanderplaats, G. N., Murman, E. M., and King, R. R., "Airfoil Section Drag Reduction at Transonic Speeds by Numerical Optimization," SAE Paper 760477, 1976.

[4]Henne, P. A., "Inverse Transonic Wing Design Method," *Journal of Aircraft*, Vol. 18, Feb. 1981, pp. 121-127.

[5]Shankar, V., "A Full Potential Inverse Method Based on a Density Linearization Scheme for Wing Design," AIAA Paper 81-1234, 1981.

[6]Jameson, A. and Cauchey, D. A., "Numerical Calculation of the Transonic Flow Past a Swept Wing," New York University, New York, ERDA Rept. C00 3077-140, 1977.

[7]Cauchey, D. A. and Jameson, A., "Numerical Calculation of Transonic Potential Flow about Wing-Body Combinations," *AIAA Journal*, Vol. 17, Feb. 1979, pp. 175-181.

[8]Barger, R. L. and Brooks, C. W., "A Streamline Curvature Method for Design of Supercritical and Subcritical Airfoils," NASA TN D-7770, 1974.

[9]Davis, W. H. Jr., "Technique for Developing Design Tools from the Analysis Methods of Computational Aerodynamics," AIAA Paper 79-1529, 1979.

[10]McFadden, G. B., "An Artificial Viscosity Method for the Design of Supercritical Airfoils," Ph.D. Thesis, New York University, New York, 1979.

[11]Heaslet, M. A. and Spreiter, J. R., "Three-Dimensional Transonic Flow Theory Applied to Slender Wings and Bodies," NACA Rept. 1318, 1957.

[12]Oswatitsch, K., "Die Geschwindigkeitsverteilung und Symmetrischen Profilen beim Auftreten Lokaler Uberschallgebiete," *Acta Physica Austrica*, Vol. 4, 1950, pp. 228-271.

[13]Nϕrstrud, H., "High Speed Flow Past Wings," NASA CR-2246, 1973.

[14]Jameson, A. and Cauchey, D. A., "A Finite Volume Method for Transonic Potential Flow Calculations," AIAA Paper 77-635, 1977.